A Piezoelectric Friction-Inertial Linear Motor Based on Piezoelectric Single-Crystal Cymbal Displacement Amplification Mechanism

Xing Xiaohong[1*], *Guo Mingsen*[2], *Chen Jialin*[2], *Wang Jiechen*[1]

1. NanHang Jincheng College, Nanjing 211156, P. R. China;
2. The State Key Laboratory of Mechanics and Control of the Mechanical Structures, Nanjing University of Aeronautics and Astronautics, Nanjing 210016, P. R. China

(Received 4 November 2015; revised 24 December 2015; accepted 25 December 2016)

Abstract: Piezoelectric friction-inertial motor is known for its promise for a long-range and high-resolution motion. The movement of the slider/rotor of the motor is achieved by stick-slip effect. We report a relaxor-based-ferroelectric-single-crystal cymbal actuator and a miniature piezoelectric friction-inertial linear motor (abbreviated as PFILM) fabricated with the cymbal actuator. The cymbal actuator is fabricated with a 10 mm diameter disk of $0.70Pb(Mg_{1/3}Nb_{2/3})O_3$-$0.30PbTiO_3$ single crystal. The displacement of the cymbal actuator increases almost proportionally from 0 to 23 μm with driving voltage up to 500 V, and the minimal hysteresis is observed. The cymbal-PFILM with 20 mm motion range works under driving voltage frequency of ca. 100 Hz to ca. 5 kHz, the fastest speed is obtained with 3.5 kHz and the no-load speed is 14 mm/s and the maximum thrust force is 98 mN. Compared with a PFILM based on multilayer piezoelectric ceramic, the proposed motor has a larger stroke under DC/quasistatic input voltage in fine motion mode, but a smaller driving force in long-travel mode due to lower resonance frequency.

Key words: piezoelectric single crystal; piezoelectric ceramic; cymbal displacement amplification mechanism; friction-inertial motor

CLC number: TM38 **Document code**: A **Article ID**: 1005-1120(2017)01-0055-07

0 Introduction

Friction-inertial motor is known for its promise for a long-range and high-resolution motion. The movement of the slider/rotor of the motor is achieved by stick-slip effect. The friction-inertial motor usually works with the piezoelectric actuator to achieve high resolution. Piezoelectric actuators refer to actuators made of piezoelectric/electrostrictive materials such as lead-Pb zirconate titanate (PZT) ceramics, lead-Pb zinconate niobate (PZN) ceramics, and lead-Pb magnesium niobate (PMN) ceramics. The piezoelectric actuator can provide motion with resolution down to sub-nanometers but with a short range (1—100 μm). Therefore, a combined piezoelectric and friction-inertial motor can achieve motion with both high resolution and long range. The high resolution and long range motion characteristics of the piezoelectric friction-inertial motor distinguish it from other types of actuators, and a literature review can be found in Ref. [1]. The accuracy is around tens of nanometers and some have a few nanometers or sub-nanometers, piezoelectric friction-inertial motors have found most applications as a micro/nanopositioner in microscopy (SEM, STM, AFM, TEM), in electrical discharge machine, optical beam deflector, nano-indentation system, and in the camera for

* Corresponding author, E-mail address: xingxh@nuaa.edu.cn.

How to cite this article: Xing Xiaohong, Guo Mingsen, Chen Jialin, et al. A piezoelectric friction-inertial linear motor based on piezoelectric single-crystal cymbal displacement amplification mechanism[J]. Trans. Nanjing Univ. Aero. Astro., 2017,34(1):55-61.

http://dx.doi.org/10.16356/j.1005-1120.2017.01.055

lens driving[2-9].

In fine motion mode[1,10], end effector (or called rotor/slider) of the piezoelectric friction-inertial motors sticks on the driving part of the piezoelectric actuator. It is desired to have a large stroke of the piezoelectric actuator. Increasing the stroke can also induce high driving speed. However, large stroke and small size of the piezoelectric actuator are mostly contradictory for application in miniature devices. Therefore, efforts are taken to utilize amplification mechanisms to enlarge the displacement of the piezoelectric actuator[11-13]. A cymbal actuator is a compact, low-cost flextensional transducer which amplifies the radial displacement of a piezoelectric disk by using two cymbal-shaped metal end caps[14-15]. Relaxor-based ferroelectric single crystal materials that exhibit extremely large piezoelectric constants ($d_{33}>2\ 500$ pC/N), electrical field induced strain ($>0.6\%$), and electromechanical coupling coefficients on the order of 90% have been reported[16]. In the present work, we fabricated a relaxor-based-ferroelectric-single-crystal cymbal actuator and characterized the performance of a piezoelectric friction-inertial linear motor fabricated with the cymbal actuator (abbreviated as cymbal-PFILM).

1 Piezoelectric Single Crystal and Cymbal Actuator

Relaxor-based ferroelectric single crystal materials achieve their ultrahigh piezoelectric properties via engineering domain states[17]. The material selected for study has a chemical composition of $0.70Pb(Mg_{1/3}Nb_{2/3})O_3$-$0.30PbTiO_3$ (abbreviated as PMN-30%PT) which is near the rhombohedral-tetragonal morphotropic phase boundary. It is a multi-domain single crystal poled along [001], which is off the spontaneous polarization direction of ⟨111⟩. We chose [001] as the thickness direction of the crystal disk because of high piezoelectric constant d_{31} as well as weak transverse anisotropy. According to the concept of domain engineering by Bell[18], the crystal exhibits macroscopic symmetry of 4 mm after poling along the [001] direction. Davis et al. utilized the physical property of single-domain PMN-33%PT single crystal and coordinate transformations, systematically calculated the effective d_{31} values[17]. The calculated results demonstrated that for the [001] poled PMN-33%PT single crystal, the d_{31} value varied slightly from $-1\ 146.1$ to $-1\ 157.6$ pC/N in the plane. We measured the piezoelectric constant d_{33} of PMN-30%PT single crystals by using a quasistatic d_{33} meter (ZJ-3AN, Institute of Acoustics, Chinese Academy of Science, Beijing, China). Single crystal samples ($d_{33}\approx 2\ 000$ pC/N) were used in this study.

The structure of fabricated cymbal actuator is shown in Fig. 1. The two end caps were fabricated with 0.2 mm-thick titanium alloy sheet by compression moulding. Titanium alloy was chosen because of its high yield strength and moderate Young's modules.

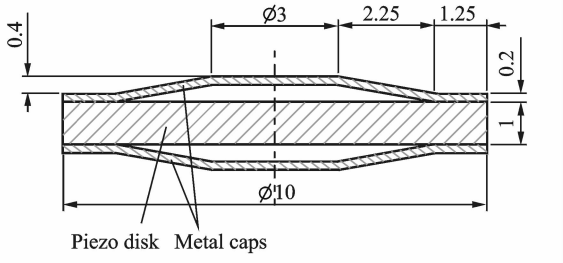

Fig. 1 Structure of the fabricated cymbal actuator

Displacement of the center of the top cap was measured using a fiber-optic sensor (MTI-2100, MTI Instruments Inc., Albany, NY), and during the measurement the cymbal actuator was placed on a table. Displacement of a cymbal actuator with varied driving voltage is plotted in Fig. 2. It is seen that the displacement increases almost proportionally from 0 to 23 μm with driving voltage up to 500 V, and the minimal hysteresis is observed. Driving voltages of 500 V to 1 000 V were applied and hysteresis appeared (the results are not shown here), and it is found that the cymbal actuator fatigued after several test cycles. It is probably micro cracks which induce the strain hysteresis and fatigue in the piezoelectric single crystal[19]. Ternary $Pb(In_{1/2}Nb_{1/2})O_3$-Pb

$(Mg_{1/3}Nb_{2/3})O_3$-$PbTiO_3$ (PIN-PMN-PT) single crystals and manganese-doping were found to show improved fatigue as well as comparable piezoelectric properties, and can be used to improve the cymbal's performance. It is noted that the displacement of the cymbal actuator can be further increased by optimizating the geometry of the metal caps.

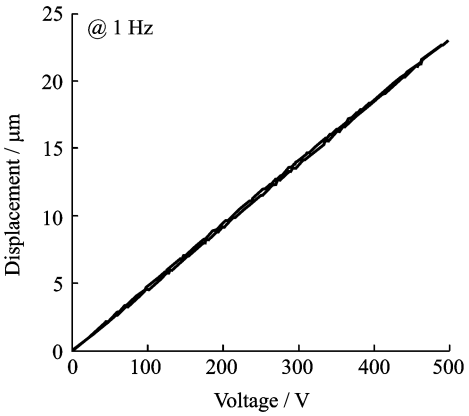

Fig. 2 Displacement of a PMN-30%PT cymbal actuator v. s. driving voltage

2 Friction-Inertial Linear Motor Based on PMN-PT Cymbal Actuator

The structure of the proposed piezoelectric friction-inertial linear motor based on cymbal actuator and the photography of the fabricated PMN-PT cymbal-PFILM are shown in Figs. 3(a) and 3(b), respectively. A carbon-fiber-reinforced-plastic shaft with 2 mm diameter and 20 mm length was glued to the top cap of the cymbal using epoxy. A slider with 1.1 g mass which consists of two divided bronze cylinders was compressed against the shaft by a rubber ring. The bottom surface of the PFILM was glued on a base for measurement. The frequency dependence of electrical impedance of the PFILM was measured by using an impedance analyzer (4294A, Agilent Technologies Inc., Santa Clara, CA), and the results are shown in Fig. 4. The frequency of the first electromechanical resonance mode is 7.7 kHz, and two spurious resonance modes at 1.5 kHz and 5.5 kHz are observed.

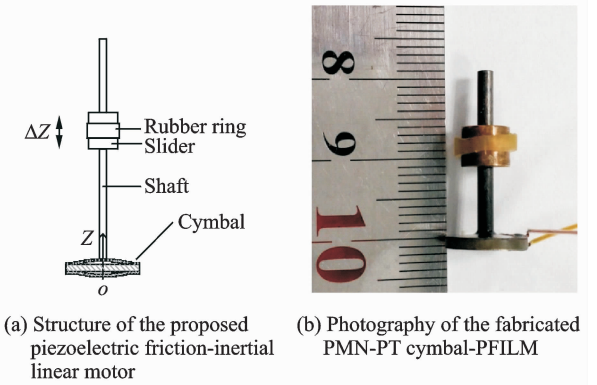

(a) Structure of the proposed piezoelectric friction-inertial linear motor (b) Photography of the fabricated PMN-PT cymbal-PFILM

Fig. 3 Structure of the proposed piezoelectric friction-inertial linear motor based on cymbal actuator, and photography of the fabricated PMN-PT cymbal-PFILM

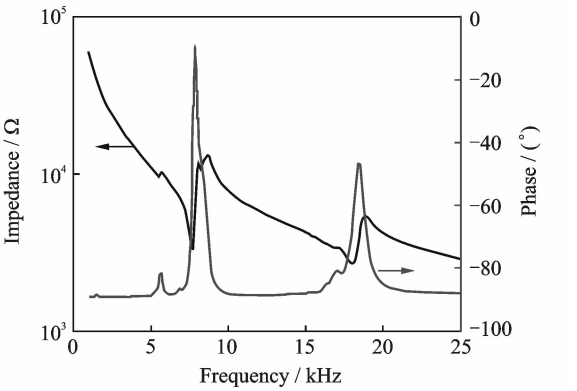

Fig. 4 Frequency dependence of electrical impedance of PMN-PT cymbal-PFILM

3 Vibration Modal Analysis by Finite Element Method

The vibration modes of the PMN-PT cymbal-PFILM were calculated by the finite element method (Ansys software, Ansys Inc., Canonsburg, PA). The piezoelectric disk was meshed with coupled-field element solid226. The metal caps and carbon-fiber-reinforced-plastic shaft were meshed with structural element solid186. Displacements of nodes on bottom surface of the PFILM were set as 0 for mechanical boundary condition. The piezoelectric and elastic properties of the PMN-30%PT single crystal are taken from Ref. [20] and listed as follows:

Density: $\rho = 8\,040\ \mathrm{kg/m^3}$

Elastic matrix in flexibility form, $\boldsymbol{s}^E$ (unit: $10^{-12}\ \mathrm{m^2/N}$)

$$\begin{bmatrix} 52 & -18.9 & -31.1 & 0 & 0 & 0 \\ -18.9 & 52 & -31.1 & 0 & 0 & 0 \\ -31.1 & -31.1 & 67.7 & 0 & 0 & 0 \\ 0 & 0 & 0 & 14 & 0 & 0 \\ 0 & 0 & 0 & 0 & 14 & 0 \\ 0 & 0 & 0 & 0 & 0 & 15.2 \end{bmatrix}$$

Piezoelectric matrix in d form (unit: pC/N)

$$\begin{bmatrix} 0 & 0 & 0 & 0 & 190 & 0 \\ 0 & 0 & 0 & 190 & 0 & 0 \\ -921 & -921 & 1\,981 & 0 & 0 & 0 \end{bmatrix}$$

Relative permittivity ($\boldsymbol{\varepsilon}^{\mathrm{T}}/\boldsymbol{\varepsilon}_0$)

$$\begin{bmatrix} 3\,600 & 0 & 0 \\ 0 & 3\,600 & 0 \\ 0 & 0 & 7\,800 \end{bmatrix}$$

The material parameters of titanium cap were set as density $\rho = 4\,850$ kg/m^3, Young's modulus $Y = 102$ GPa, and Poisson's ratio $\sigma = 0.3$. For carbon-fiber-reinforced-plastic shaft, $\rho = 1\,497$ kg/m^3, $Y = 181$ GPa, and $\sigma = 0.3$.

Fig. 5 shows the first three resonance modes of the PFILM. The two modes at 1.59 kHz (Fig. 5(a)) and 5.83 kHz (Fig. 5(b)) corresponding to the two spurious modes in Fig. 4 are bending vibration modes, which can be eliminated by clamping the free end of the shaft with damping rubber. The mode at 8.61 kHz (Fig. 5(c)) corresponds to the main electromechanical resonance mode at 7.7 kHz in Fig. 4, the difference between the calculated and measured resonance frequencies is due to inaccuracy of materials parameters for simulation and geometric deviation in fabrication. Compared with a PFILM based on multilayer piezoelectric ceramic[10,21], the PMN-PT cymbal-PFILM has a larger displacement under DC/quasistatic input voltage, but a lower resonance frequency, which leads to a smaller transient acceleration (i.e. a smaller driving force) under step input voltage.

4 Performance of PMN-PT Cymbal-PFILM

The performance of the PMN-PT cymbal-PFILM was then characterized by setup as shown in Fig. 6. A 5 V-sawtooth signal output by a function generator is amplified by a high-voltage amplifier (BOP 1 000M, Kepco Inc., NY) and then applied to the actuator. The load was applied by hanging a mass via a pulley. The average velocity of the slider was obtained by measuring the travel distance and time. It is noted that velocity of the slider varied slightly along the shaft[22-23].

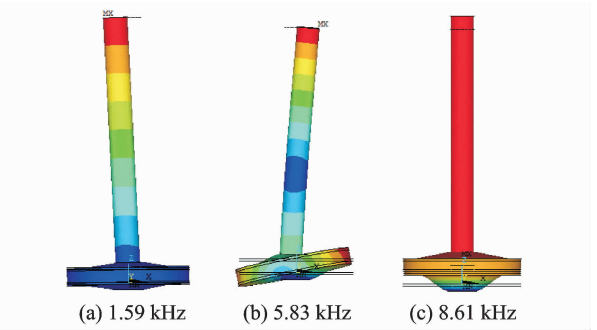

Fig. 5 The calculated first three resonance modes of PFILM at different frequencies

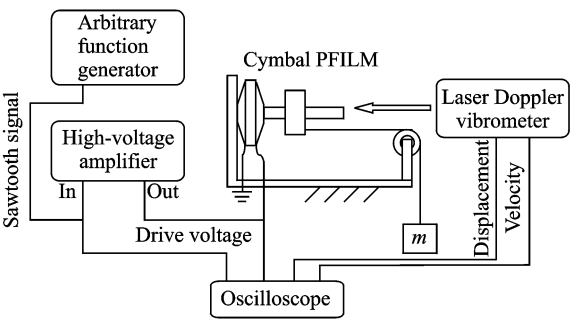

Fig. 6 Experiment setup for measurement of cymbal-PFILM

The actuator works with driving voltage frequency of ca. 100 Hz to ca. 5 kHz, the fastest speed was obtained with 3.5 kHz and the corresponding speed-load characteristics of the actuator is shown in Fig. 7. An appropriate pre-stressing force between the slider and the shaft was provided by the rubber ring, the static friction force was measured to be 0.84 N, the no-load speed was 14 mm/s and the maximum thrust force was 98 mN. The performance of the actuator can be further enhanced by optimizing the pre-stressing force and slider-shaft frictional interface.

A laser Doppler vibrometer (OFV505, Polytec GmbH, Waldbronn, Germany) was utilized to measure the vibration of the shaft end of the PFILM as well as the movement of the slider.

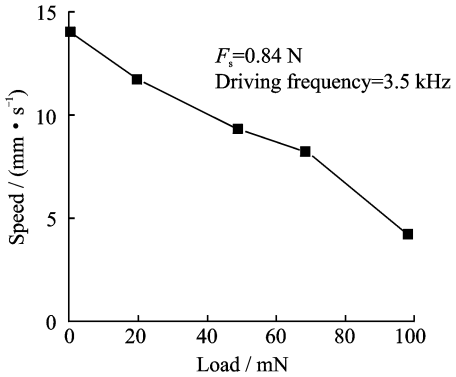

Fig. 7 The measured speed-load characteristics of PMN-PT cymbal-PFILM

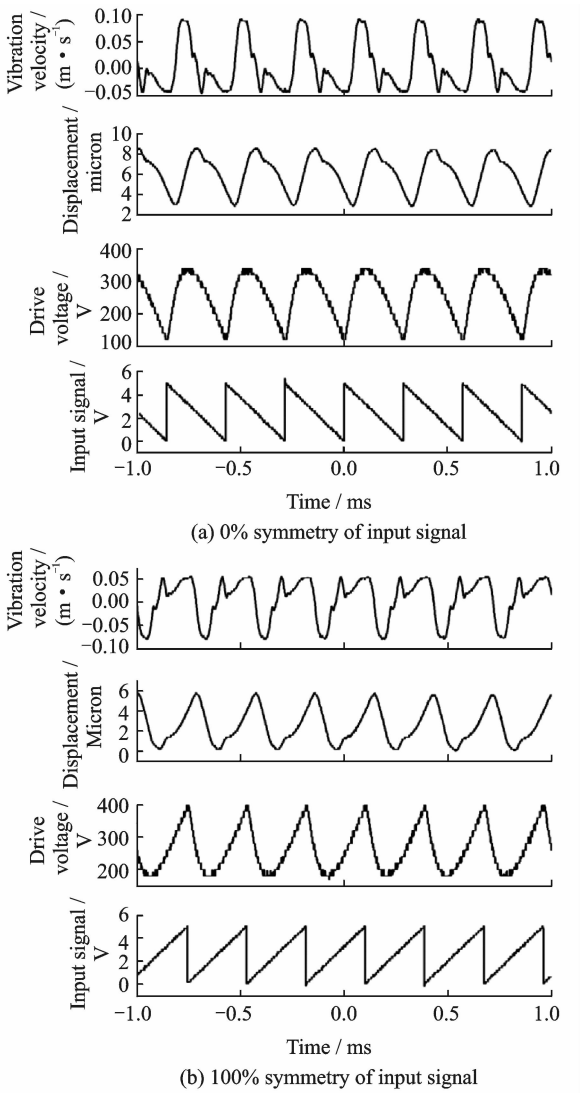

Fig. 8 Vibration characteristics of shaft of PMN-PT cymbal-PFILM in response to sawtooth driving voltages with 3.5 kHz frequency

Fig. 8 shows the vibration characteristics of the shaft end in response to sawtooth driving voltages. Due to the frequency bandwidth and current limitation of the voltage amplifier, the drive voltage distorts slightly from ideal sawtooth waveform. The displacement of the shaft follows the drive voltage waveform. The characteristics are desirable to have the inertia properties for the actuator, which means that the shaft rises slowly in one direction and falls rapidly in the opposite. The measured amplitude of displacement is 5.8 μm with a sawtooth drive voltage of 260 V (peak-to-peak value), as shown in Fig. 8. The displacement of the shaft with a 100 Hz triangle driving voltage of 500 V was measured to be 11.4 μm (not shown here), which is smaller than quasistatic displacement (23 μm) of PMN-PT cymbal under a free boundary condition. The epoxy on top and bottom surfaces of the cymbal used for assembly induces the decrease of displacement, and reducing the top/bottom surface areas will mitigate this problem.

Fig. 9 shows the movement of the slider under sawtooth input signal with 0% symmetry, no load was applied during the measurement. The operation of the PFILM is stable after the initial 1—2 pulse cycles, and the average step distance per pulse is 4.4 μm. The operation of the PFIA was not stable when using 1 or 2 pulse cycles. The reason may be in the first cycle, the inertial force is not large enough to overcome the static friction force. Since the maximum displacement of the PFIA in DC (or quasistatic) mode, 11.4 μm is larger than the average step distance, fast and precise positioning with nanometer precision in closed-loop control can be achieved.

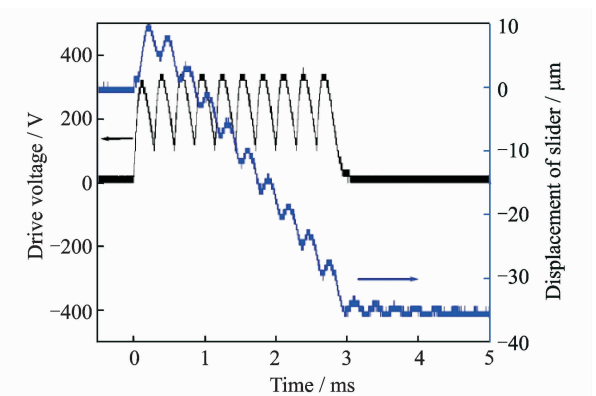

Fig. 9 Movement of the slider under sawtooth input signal

5 Conclusions

We have fabricated a relaxor-based-ferroelectric-single-crystal cymbal actuator and characterized the performance of a miniature PFILM fabricated with the cymbal actuator. The cymbal actuator was fabricated with a 10 mm diameter disk of $0.70Pb(Mg_{1/3}Nb_{2/3})O_3$-$0.30PbTiO_3$ single crystal. The displacement of the cymbal actuator increases almost proportionally from 0 to 23 μm with driving voltage up to 500 V, and minimal hysteresis is observed. The cymbal-PFILM with 20 mm motion range works under driving voltage frequency of about 100 Hz to about 5 kHz. The fastest speed is obtained with 3.5 kHz. And the no-load speed is 14 mm/s and the maximum thrust force is 98 mN. The measured and calculated electromechanical resonance frequencies of the PFILM are 7.7 kHz and 8.61 kHz, respectively. Compared with a PFILM based on multilayer piezoelectric ceramic, the PMN-PT cymbal-PFILM has a larger displacement under DC/quasistatic input voltage in fine motion mode, but a smaller driving force in long-travel mode due to lower resonance frequency. The PMN-PT cymbal-PFILM has potential to be applied to miniature devices, such as in endoscope for actuating the confocal laser endomicroscope probe.

Acknowledgements

The authors would like to thank Prof. Haosu Luo for providing the piezoelectric single crystals. This work was supported by the National Natural Science Foundation of China (No. 51105193), the Natural Science Foundation of Jiangsu Province (No. BK20131362), the Priority Academic Program Development of Jiangsu Higher Education Institutions, and Jiangsu Students' Platform for Innovation and Entrepreneurship Training Program (No. 201613655016X).

References:

[1] ZHANG Z M, AN Q, LI J W, et al. Piezoelectric friction-inertia actuator—A critical review and future perspective [J]. International Journal of Advanced Manufacturing Technology, 2012,62(5/6/7/8):669-685.

[2] KATSUMI O. Lens unit: JP2006113155[P]. 2006-04-27.

[3] PAIK D S, YOO K H, KANG C Y, et al. Multilayer piezoelectric linear ultrasonic motor for camera module[J]. Journal of Electroceramics, 2009,22(1/2/3):346-351.

[4] ZHANG Z G, UENO T, HIGUCHI T. Development of a magnetostrictive linear motor for microrobots using Fe-Ga (Galfenol) alloys[J]. IEEE Transactions on Magnetics, 2009,45(10):4598-4600.

[5] OH C H, CHOI J H, NAM H J, et al. Ultra-compact, zero-power magnetic latching piezoelectric inchworm motor with integrated position sensor[J]. Sensors and Actuators A: Physical, 2010,158(2):306-312.

[6] LEE J, KWON W S, KIM K S, et al. A novel smooth impact drive mechanism actuation method with dual-slider for a compact zoom lens system[J]. Review of Scientific Instruments, 2011, 82(8): 085105.

[7] MORITA T, MURAKAMI H, YOKOSE T, et al. A miniaturized resonant-type smooth impact drive mechanism actuator[J]. Sensors and Actuators A: Physical, 2012,178:188-192.

[8] NISHIMURA T, HOSAKA H, MORITA T. Resonant-type smooth impact drive mechanism (SIDM) actuator using a bolt-clamped Langevin transducer [J]. Ultrasonics, 2012,52(1):75-80.

[9] MAZEIKA D, VASILJEV P. Linear inertial piezoelectric motor with bimorph disc[J]. Mechanical Systems and Signal Processing, 2013,36(1):110-117.

[10] MORITA T, YOSHIDA R, OKAMOTO Y, et al. Three DOF parallel link mechanism utilizing smooth impact drive mechanism[J]. Precision Engineering, 2002,26(3):289-295.

[11] CHANG S H, LI S S. A high resolution long travel friction-drive micropositioner with programmable step size[J]. Review of Scientific Instruments, 1999, 70(6):2776-2782.

[12] WANG Y C, CHANG S H. Design and performance of a piezoelectric actuated precise rotary positioned [J]. Review of Scientific Instruments, 2006,77(10): 105101-1-5.

[13] CLAEYSSEN F, DUCAMP A, BARILLOT F, et al. Stepping piezoelectric actuators based on APAs [C]// ACTUATOR 2008, 11th International Conference on New Actuators. Bremen, Germany, 2008: 623-626.

[14] DOGAN A, UCHINO K, NEWNHAM R E. Composite piezoelectric transducer with truncated conical endcaps cymbal[J]. IEEE Transactions on Ultrasonics, Ferroelectrics, and Frequency Control, 1997,44(3):597-605.

[15] MEYER Jr. R J, DOGAN A, YOON C, et al. Displacement amplification of electroactive materials using the cymbal flextensional transducer[J]. Sensors and Actuators A, 2001,87(3):157-162.

[16] PARK S E, SHROUT T R. Ultrahigh strain and piezoelectric behavior in relaxor based ferroelectric single crystals[J]. Journal of Applied Physics, 1997,82(4):1804-1811.

[17] DAVIS M, DAMJANOVIC D, HAYEM D, et al. Domain engineering of the transverse piezoelectric coefficient in perovskite ferroelectrics[J]. Journal of Applied Physics, 2005,98(1):014102-1-9.

[18] BELL A J. Phenomenologically derived electric field-temperature phase diagrams and piezoelectric coefficients for single crystal barium titanate under fields along different axes[J]. Journal of Applied Physics, 2001,89(7):3907-3914.

[19] ZHANG S, LUO J, LI F, et al. Polarization fatigue in $Pb(In_{0.5}Nb_{0.5})O_3$-$Pb(Mg_{1/3}Nb_{2/3})O_3$-$PbTiO_3$ single crystals[J]. Acta Materialia, 2010,58(10):3773-3780.

[20] CAO H, HUGO SCHMIDT V, ZHANG R, et al. Elastic, piezoelectric, and dielectric properties of 0.58Pb$(Mg_{1/3}Nb_{2/3})O_3$-0.42$PbTiO_3$ single crystal[J]. Journal of Applied Physics, 2004,96(1):549-554.

[21] OKAMOTO Y, YOSHIDA R. Development of linear actuators using piezoelectric elements[J]. Electronics and Communications in Japan, Part 3, 1998, 81(11):11-17.

[22] KANG C Y, YOO K H, KO H P, et al. Analysis of driving mechanism for tiny piezoelectric linear motor [J]. Journal of Electroceramics, 2006,17(2/3/4): 609-612.

[23] KO H P, KIM S, BORODINAS S N, et al. A novel tiny ultrasonic linear motor using the radial mode of a bimorph[J]. Sensors and Actuators A: Physical, 2006,125(2):477-481.

Ms. **Xing Xiaohong** was born in 1980 at Liaoning, China. She received the B. E. degree in Aircraft Manufacturing Engineering and M. E. degree in Manufacturing Engineering of Aerospace from Nanjing University of Aeronautics and Astronautics (NUAA), Nanjing, China, in 2003 and 2008, respectively. She is currently a lecturer at Nanhang Jincheng College, Nanjing, China. Her main research field is NC processing technology and mold design and manufacture.

Dr. **Guo Mingsen** was born in 1980 at Hubei, China. He received the B. Sc. degree in Physics, M. Sc. degree in Physics of Condensed Matter, and Ph. D. degree in physics and chemistry of materials from Wuhan University, Wuhan, China, in 2002, 2005, and 2008, respectively. He is currently an associate professor at NUAA. Prior to joining NUAA, he was a postdoctoral fellow at Peking University, Beijing, China. From December 2005 to October 2007, he was a research assistant at Hong Kong Polytechnic University, HK SAR, China. His main research interests include piezoelectric materials, sensors, and actuators.

Mr. **Chen Jialin** was born in 1992 at Hunan, China. He received the B. Sc. degree in Physics from NUAA, in 2014. And now he is a graduate student major in mechanical design and theory in NUAA.

Mr. **Wang Jiechen** was born in 1996 in Jiangsu, China. He is an undergraduate student major in mechanical engineering in Nanhang Jincheng College, Nanjing, China.

(Executive Editor: Zhang Tong)